Journal of Power Sources 248 (2014) 434–438

Contents lists available at ScienceDirect

Journal of Power Sources

journal homepage: www.elsevier.com/locate/jpowsour

Short communication

Energy storage via polyvinylidene fluoride dielectric on the counterelectrode of dye-sensitized solar cells

Xuezhen Huang, Xi Zhang, Hongrui Jiang*

Materials Science Program, Department of Electrical and Computer Engineering, University of Wisconsin–Madison, Madison, WI 53706, USA

HIGHLIGHTS

- Photovoltaic self-charging cells (PSCs) for combined energy conversion and storage.
- PVDF dielectric layer contributes significantly to the energy storage capability.
- Discontinuous ultrathin Au quasi-electrode is key to success of highly compact PSCs.

GRAPHICAL ABSTRACT

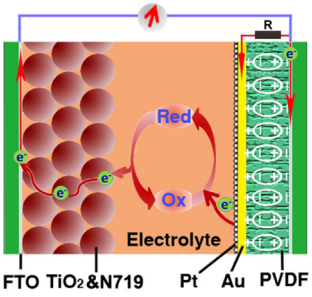

ARTICLE INFO

Article history:
Received 23 July 2013
Received in revised form
18 September 2013
Accepted 21 September 2013
Available online 2 October 2013

Keywords:
PVDF film
Dye-sensitized solar cells
Energy storage
Self-charging

ABSTRACT

To study the fundamental energy storage mechanism of photovoltaically self-charging cells (PSCs) without involving light-responsive semiconductor materials such as Si powder and ZnO nanowires, we fabricate a two-electrode PSC with the dual functions of photocurrent output and energy storage by introducing a PVDF film dielectric on the counterelectrode of a dye-sensitized solar cell. A layer of ultrathin Au film used as a quasi-electrode establishes a shared interface for the I^-/I_3^- redox reaction and for the contact between the electrolyte and the dielectric for the energy storage, and prohibits recombination during the discharging period because of its discontinuity. PSCs with a 10-nm-thick PVDF provide a steady photocurrent output and achieve a light-to-electricity conversion efficiency (η) of 3.38%, and simultaneously offer energy storage with a charge density of 1.67 C g^{-1}. Using this quasi-electrode design, optimized energy storage structures may be used in PSCs for high energy storage density.

1. Introduction

Recently, dielectric polymers for energy storage have attracted considerable attention because of their relatively high energy density, high reliability, low dielectric loss, high speed, and low cost [1–4]. Polyvinylidene fluoride (PVDF) has a high dielectric constant, a high electric displacement field (>0.1 C m^{-2}) and excellent chemical corrosion resistance, and has been widely used as a binder in energy storage systems such as lithium ion batteries and supercapacitors. With the development of solar energy harvesting and the increasing demand for compact, low-cost electrical power devices, a new type of photovoltaic cell, photovoltaically self-charging cells, or PSCs, have gained attention, since they combine the functions of energy conversion and energy storage in a single device [5–11]. To hybridize a solar cell and an energy storage element, typical strategies reported to date include dye-sensitized solar cell (DSSC)/Li battery, DSSC/supercapacitor and organic photovoltaics/supercapacitor, mostly with a three-electrode design, which is equivalent to combining two separate devices together. For PSCs with more compact structures (in a two-electrode mode),

* Corresponding author.
E-mail addresses: hongrui@engr.wisc.edu, hongruijiang@wisc.edu (H. Jiang).

0378-7753/$ – see front matter © 2013 Elsevier B.V. All rights reserved.
http://dx.doi.org/10.1016/j.jpowsour.2013.09.094

it remains a challenge to obtain a continuous power output after being fully charged under steady illumination and higher photoelectric conversion efficiency [12].

Previous work in our group reported that PVDF/Si powder composites could be used as active materials to fabricate a two-electrode DSSC-like photocapacitor, which showed high photoresponse, rechargeability, and long-term storage properties [10]. It implied that the two parts of the PSC can share a single electrolyte, and the dielectric material-functionalized counterelectrode (CE) permits energy storage. This concept has been further developed in our latest work, in which we used PSCs with PVDF/ZnO nanowire nanocomposite-modified CEs for energy storage [13]. However, a PVDF/Si photoelectrode can harvest energy, since it generates an open circuit voltage of 0.47 V under solar irradiation. This complicates the role of a PVDF dielectric film for energy storage [10]. In this work, TiO_2 DSSCs with CEs functionalized only by a PVDF dielectric were fabricated. They showed comparable energy conversion and storage capability to those in Ref. [13]. The stored charge density was up to 1.67 C g^{-1} based on the mass of PVDF, while the highest light-to-electricity conversion efficiency (η) achieved for such a cell after being fully charged could be up to 3.38%. This work indicates that the ultra-thin Au film can be used to control the recombination of charges in the discharge process due to its discontinuity, without destroying the quasi-electrode role in the energy conversion process. Such cells have potential in the development of low-power consumption devices, which can satisfy demand for continuous and unattended power supply.

2. Experimental

2.1. Materials and PSC fabrication

The CEs of PSC were prepared first by dip-coating 2, 10, 20 μL, respectively, of PVDF (Kynar 301F, Mw = 3.8 × 10^5, Arkema, USA)/dimethylsulfoxide (DMSO, Aldrich, USA) solution (1.5 g PVDF/100 g DMSO) onto FTO substrates (1.5 cm × 2 cm, TEC-15, MTI Co., USA), followed by drying at 90 °C in air for 30 min. The thicknesses of PVDF were correspondingly 2 μm, 10 μm and 20 μm, as confirmed by a surface profilometer (Tencor AlphaStep 200, Brumley South, Inc. Mooresville, USA). A 15-nm-thick Au layer was subsequently sputtered onto the surface of the PVDF by a Denton sputter coater Desk II. Then, a Pt layer was deposited onto the Au surface of the CE by a 2-min electrodeposition process in chloroplatinic acid (H_2PtCl_6; Aldrich, USA) solution (0.5 M). Photoelectrodes were prepared by doctor-blade coating of a TiO_2-containing viscous paste (Solaronix, 15–20 nm particles, Switzerland) onto the FTO substrate, followed by sintering at 500 °C for 1 h. After being cooled to 120 °C, the films were immersed into a 0.3 mM solution of ruthenium complex N719 dye (Solaronix, Aubonne, Switzerland) in dry ethanol for 24 h. The photoelectrodes and the CEs had the same active area of 0.25 cm^2. TiO_2 photoelectrode and CE were assembled together by 50-μm spacer (Surlyn, Aubonne, Solaronix, Switzerland). The internal space of the cell was filled with a liquid electrolyte [0.05 M LiI, 0.03 M I_2, 0.1 M guanidinium thiocyanate (GNCS), 1.0 M 1,3-dimethylimidazolium iodide (DMII), 0.5 M 4-tertbutyl pyridine (TBP) in 3-methoxyproionitrile and acetonitrile (6:4)].

2.2. Instrumentation

The morphology of PVDF film was characterized by an SEM (Zeiss LEO 1530 containing a detector with a resolution of 129 eV at manganese and a light element detection limit of boron). The XRD spectrum of PVDF film was measured by a Bruker/Siemens Hi-Star 2d X-ray Diffractometer with a monochromatic Cu K-alpha point source (0.8 mm). *J–V* performance was tested by using a Keithley 2400 source meter under AM 1.5G simulated sunlight (Newport 94022A equipped with a 150 W Xe lamp and AM 1.5G filter). The photovoltage and photocurrent transient curves (*V–t*, *J–t*) measurements were carried out by an Agilent 34411A $6_{1/2}$ digital multimeter. The PSCs were illuminated under AM 1.5G for about 5 min before the light source was turned off for discharging measurements: through a 1 MΩ resistor for *V–t*; in short-circuit for *J–t*.

3. Results and discussion

3.1. Working mechanism

Fig. 1 shows that the majority of the photon-generated current passes through a quasi-electrode consisting of Pt/Au layer on the surface of the PVDF film to the interface of Pt atoms and the electrolyte under certain resistance (represented by resistor *R*) for the photoelectric conversion; the rest of the charge accumulates on the surface of the fluorine-doped tin oxide (FTO) electrode, giving energy storage. Part of the Li^+ in the electrolyte may be attracted onto the Pt surface through the electric polarization of PVDF by the electrons on the other side. To establish the I^-/I_3^- redox reaction interface, a quasi-electrode was introduced to the two-electrode PSC by forming a layer of Pt/Au coating on the top of PVDF dielectric as shown in Fig. 1. The sputtered Au layer is to provide the electroconductivity on the surface of PVDF coating for Pt electrodeposition. We observed in our experiments that the Au layer alone showed very poor catalysis for the I^-/I_3^- redox reaction. Moreover, the electronic properties of ultrathin Au films deposited on a substrate are mainly associated with the discontinuous film morphology and its effect on electronic transport [14–17]. The film surface generally develops from granules, islands, mazes, and continuous structures with the increasing film thickness, thus undergoing an insulator-to-metal transition. For a smooth and continuous conducting film, both quantum and classical size effects dominate the conductivity. In the insulating phase, the conduction electrons are confined to the metal islands and electrical conduction can only occur via thermally activated hopping or tunneling between the grains, which requires the electrons to percolate through the random network of conducting channels [14]. The discontinuity of PVDF/ZnO nanowire nanocomposite has been discussed in Ref. [13]. However, it is not clear on if the porous network formed in PVDF/ZnO nanowire nanocomposite also contributes to the discontinuity. In this work, the prestine PVDF film

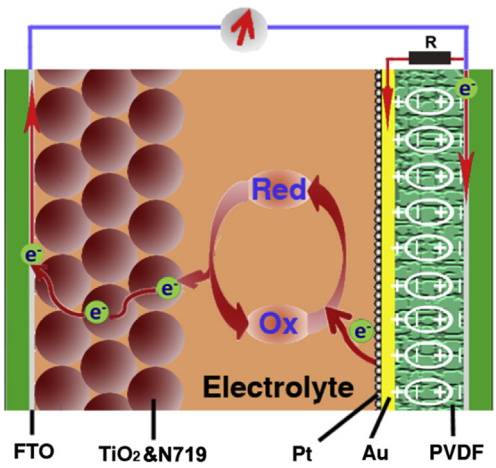

Fig. 1. Schematic of the structure and mechanism of TiO_2 DSSC with energy storage function by modifying the CE with PVDF dielectric.

without porous structures, confirmed by SEM, indicates that the discontinuity should be attributed to the ultra-thin Au film. We establish the 15 nm ultrathin Pt/Au film quasi-electrode to avoid a "short" circuit and use a resistor or R in Fig. 1 to represent the connection between the FTO and Pt/Au layer.

3.2. Performance of PSCs

When the PSC is irradiated, photo-generated electrons from the photoelectrode pass through the external circuit to the CE. One portion of the electrons reaches the Au/Pt layer and reduces I_3^- anions to maintain the operation of DSSC. The rest of the charge remains on the PVDF and FTO interface and contributes to the binding of the opposite charge at PVDF/electrolyte interface under the oriented external bias dipoles as shown in Fig. 1. Fig. 2 shows the SEM images of ultra-thin Pt/Au coated dielectric. The morphology of Au grains and cracks is independent of the thickness of PVDF film and similar to those reported previously [14,15]. The mixed β phase peak at 20.05° XRD spectrum of PVDF film (Fig. S1) indicates that the crystalline structure of PVDF film dried at 90 °C is mainly α phase, corresponding to negligible ferroelectric properties in the PVDF film [18].

Fig. 3 shows the light to electricity conversion efficiency of a pure DSSC and PSCs with different thicknesses of PVDF dielectric. The pure DSSC shows the highest η (up to 7.32%). When the CE was modified by PVDF nanocomposites, η dropped to between 1.33% and 3.38%, with η depending on the thickness of PVDF. Compared with a pure DSSC, the higher open circuit voltages of PSCs indicate lower electron ejection efficiencies from ultrathin Pt/Au films. The performance of the PSCs with 10-μm-thick PVDF was greater than those with other thicknesses. Thicker or thinner PVDF layers could reduce the photovoltaic performance of corresponding DSSCs. In PSCs without Pt deposition on the Au thin film, the energy conversion efficiency was much lower than 1%.

The energy storage capability of PSCs is shown by the discharging photovoltage transient (J–t) curves in Fig. 4a. The photocurrent of samples with Pt catalyst decreased mildly to an equilibrium value from the highest initial values within several tens of seconds under illumination, rather than to a very low value sharply that causes poor photo-generated current output (<1%) [6,8,10]. The PSC with a 10 μm thickness PVDF film gave an energy storage capacity of 1.67 C per gram of PVDF, which was on the order of 15 times larger than that of samples with 20 μm and 2 μm thickness PVDF films. Cells with a 2 μm thickness PVDF film had a higher η and the same energy storage capacity per gram of PVDF compared to that for a 20 μm film. This indicates that thinner PVDF dielectric is preferred to attain better charge capacity performance, which is consistent with the relationship between the electrostatic capacity of a capacitor and the thickness (d) of its dielectric: $C \propto \varepsilon/d$,

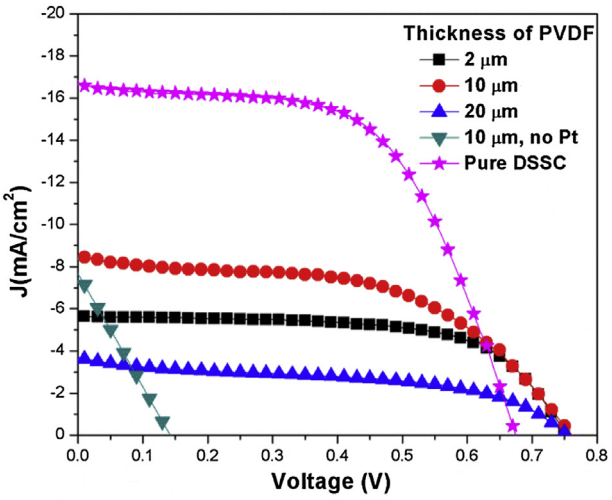

Fig. 3. J–V curves of PSCs with different PVDF thicknesses compared with a simple DSSC.

where ε is the dielectric constant. The photocurrent of a PSC without a Pt coating increases somewhat, which indicates a lower electron injection efficiency than that in PSCs with a Pt catalyst at the electrolyte/catalyst interface. However, the absence of a Pt layer decreases the discharge slope, as shown in Fig. 4a, due to a slower recombination rate, and contributes to an energy storage capacity per gram of PVDF which is 8 times higher than that of samples with 20 μm and 2 μm thick PVDF films. Such results imply the feasibility to pursue various balances between the two functions of the PSC by changing the CE parameters.

Although the ultrathin Pt/Au films on varying PVDF thicknesses have the same morphology, energy dispersion X-ray (EDX) spectra in Fig. S2 show that the Pt composition with respect to the same thickness of Au film is 23%, 18% and 7% for PVDF film thicknesses of 2 μm, 10 μm and 20 μm, respectively. The higher Pt loading may contribute to higher η. However, an attenuated PVDF film may result in dielectric discontinuity, resulting in non-uniform Pt distribution on CEs during electrodeposition, giving a reduced catalytic effect and photovoltaic efficiency (Fig. S3).

The V–t curves of PSCs are shown in Fig. 4b. The discharge voltage polarity of each PSC was reversed compared with its photovoltage, indicating that the discharging voltage was from the capacitor section. The PSC without Pt catalyst only had a very small initial discharge voltage (-8×10^{-5} V), resulting from its low photovoltaic efficiency. In contrast, its discharge current was comparable to that of the best PSC, with an initial peak possibly because of the rapid transfer of electrons accumulated on the non-

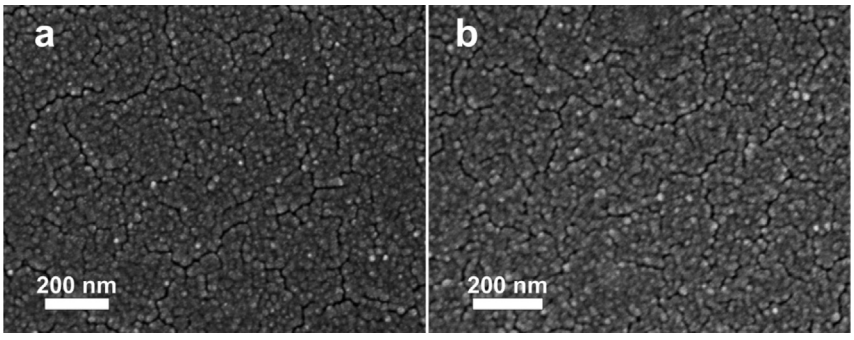

Fig. 2. SEM images of the morphology of 15 nm-thick Pt/Au ultrathin film coated on (a) 2 μm PVDF film; (b) 20 μm PVDF film.

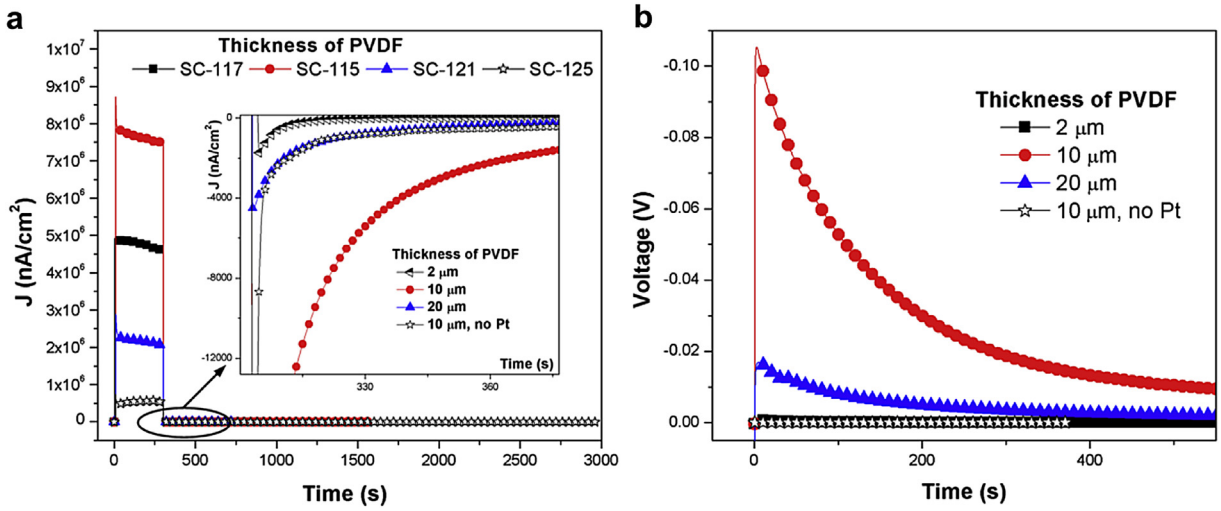

Fig. 4. (a) Charge and discharge J–t curves of PSCs. Inset in (a): discharge curves zoomed in. (b) Open-circuit voltage of PSCs as a function of discharging time.

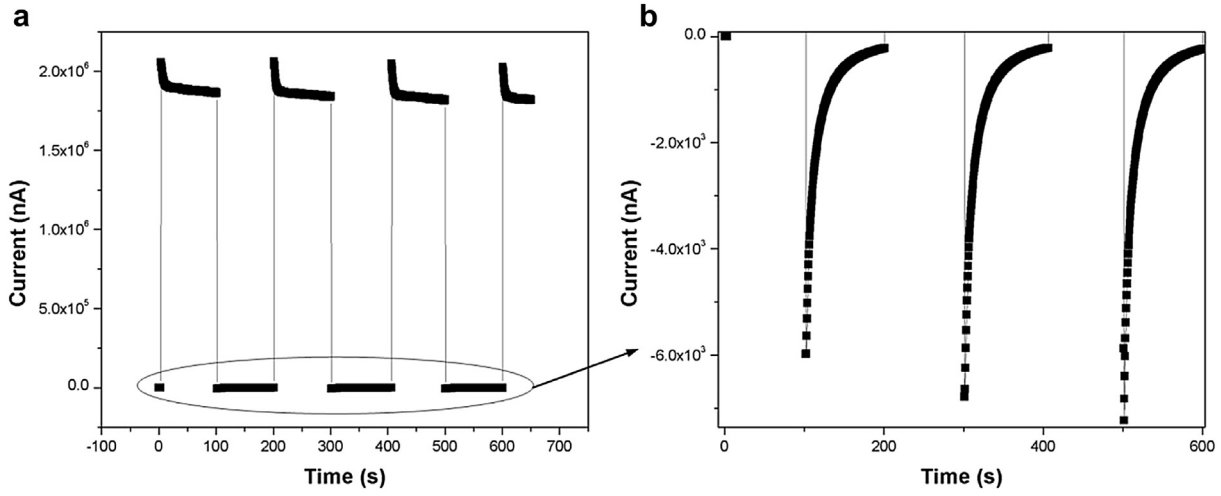

Fig. 5. (a) Change of photocurrent with time for a PSC under interrupted illumination. (b) Discharge curves zoomed in.

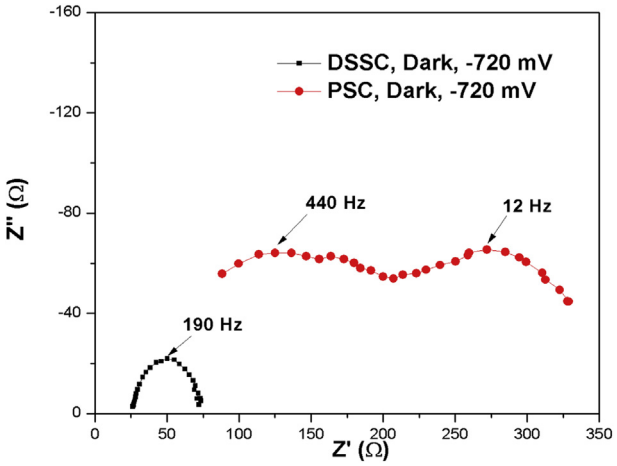

Fig. 6. Electrochemical impedance spectroscopy (Nyquist plots) of a PSC and a DSSC with a frequency loop from 1000 Hz to 1 Hz using a perturbation amplitude of 5 mV and −0.720 V bias at the open potential.

Pt coated Au surface, as shown in the inset in Fig. 4a. Fig. 5 shows the good repeatability of the PSCs in photo-charging and discharging cycles. The increasing initial maximum of discharge current as a function of cycle number shown in Fig. 5b demonstrates that this was due to the charge remaining from the last charge–discharge cycle when the discharge was not complete. Electrochemical impedance spectroscopy (EIS) measurements were carried out by a BAS 100B electrochemical analyzer (Bioanalytical Systems, Inc., W. Lafayette, IN). Fig. 6 shows that a PSC possesses two circular arcs under a frequency loop from 1000 Hz to 1 Hz, instead of a semicircle usually observed in the EIS of DSSCs. Comparing the respective frequency where the highest Z″ values appeared in the EIS of a DSSC and a PSC, we attribute the extra circular arc at the high frequency end to the PVDF dielectric/Au/Pt interface, which has been represented with a resistance in Fig. 1. According to Fig. 6, PSCs have higher internal resistance than DSSCs due to a PVDF dielectric, which causes a relatively lower η.

4. Conclusion

We have demonstrated a two-electrode PSC with the dual-functions of photocurrent output and energy storage by applying

a PVDF dielectric film on the counterelectrode (CE). With a 10 nm PVDF layer, it could provide a steady photocurrent output with η of 3.38%, and could offer simultaneous energy storage of 1.67 C g^{-1}. A thinner PVDF film is preferred for better performance in both modes. The ultrathin discontinuous Au film used establishes a shared interface for I^-/I_3^- redox reaction and for contact between the electrolyte and the dielectric film for energy storage. Energy storage structures, such as a porous electrode in an electrochemical supercapacitor, may be applied to give high energy storage densities.

Acknowledgments

This work was supported by the US National Institute of Health (Grant No. 1DP2OD008678). This research utilized NSF supported shared facilities at the University of Wisconsin.

Appendix A. Supplementary data

Supplementary data related to this article can be found at http://dx.doi.org/10.1016/j.jpowsour.2013.09.094.

References

[1] B.J. Chu, X. Zhou, K. Ren, B. Neese, M. Lin, Q. Wang, F. Bauer, Q.M. Zhang, Science 313 (2006) 334–336.
[2] Y. Cao, P.C. Irwin, K. Younsi, IEEE Trans. Dielectr. Elect. Insul. 11 (2004) 797–807.
[3] V. Tomer, E. Manias, C.A. Randall, J. Appl. Phys. 110 (2011) 044107.
[4] K. Yao, S. Chen, M. Rahimabady, M.S. Mirshekarloo, S. Yu, F.E.H. Tay, T. Sritharan, L. Lu, IEEE Trans. Ultrason. Ferroelectr. Freq. Control 58 (2011) 1968–1974.
[5] T. Song, B. Sun, ChemSusChem. 6 (2013) 408–410.
[6] T. Miyasaka, T.N. Murakami, Appl. Phys. Lett. 85 (2004) 3932–3934.
[7] H.-W. Chen, C.-Y. Hsu, J.-G. Chen, K.-M. Lee, C.-C. Wang, K.-C. Huang, K.-C. Ho, J. Power Sources 195 (2010) 6225–6231.
[8] T.N. Murakami, N. Kawashima, T. Miyasaka, Chem. Commun. 26 (2005) 3346–3348.
[9] W. Guo, X. Xue, S. Wang, C. Lin, Z. Wang, Nano Lett. 12 (2012) 2520–2523.
[10] C. Lo, C. Li, H. Jiang, AIP Adv. 1 (2011) 042104.
[11] G. Wee, T. Salim, Y.M. Lam, S.G. Mhaisalkara, M. Srinivasan, Energy Environ. Sci. 4 (2011) 413–416.
[12] A. Morales-Acevedo, Appl. Phys. Lett. 86 (2005) 196101.
[13] X. Zhang, X. Huang, C. Li, H. Jiang, Adv. Mater. 25 (2013) 4093–4096.
[14] Y. Poo, R. Wu, X. Fan, J.Q. Xiao, Rev. Sci. Instrum. 81 (2010) 064701.
[15] M. Walther, D.G. Cooke, C. Sherstan, M. Hajar, M.R. Freeman, F.A. Hegmann, Phys. Rev. B 76 (2007) 125408.
[16] P. Sheng, B. Abeles, Y. Arie, Phys. Rev. Lett. 31 (1973) 44–47.
[17] P. Sheng, Z.-Q. Zhang, J. Phys. Condens. Matter 3 (1991) 4257–4267.
[18] W. Ma, J. Zhang, S. Chen, X. Wang, J. Macromol. Sci. B. 47 (2008) 434.